Korea-Australia Rheology Journal
Vol. 15, No. 1, March 2003 pp. 35-41

Dilatant flow characteristics model of coarse particle suspensions with uniform size distribution

Shinichi Ookawara* and Kohei Ogawa
Department of Chemical Engineering, Graduate School of Science and Engineering, Tokyo Institute of Technology, Tokyo 152-8552, Japan
(Received December 27, 2002)

Abstract

It is expected that particle size distribution of any portion obtained through screening, is of more uniform than that of the original mixture, typically following such as log-normal, Rosin-Rammler distributions and so on. In this study, therefore, a new relation between parameters of the uniform distribution and flow characteristics of the coarse particle suspensions is derived based on the continuous polydisperse model (Ookawara and Ogawa, 2002b), which is derived from the discrete polydisperse model (Ookawara and Ogawa, 2002a). The derived model equation predicts a linear increase of viscosity with shear rate, viz., dilatant flow characteristics. Further, the increase of viscosity is expected to be proportional to the square of volume fraction of particles, and to show the linear dependency on density and average diameter of particles. It is also shown that the uniform distribution model includes additional term that expresses the effect of distribution width. For verification of the model, the experimental results of Clarke (1967) are cited as well as in our previous work for the monodisperse model (Ookawara and Ogawa, 2000) since most parameters were varied independently in his work. It is suggested that the newly introduced term expands the applicable range compared with the monodisperse model.

Keywords : shear thickening, dilatancy, suspension viscosity, particle size distribution, monodisperse, polydisperse

1. Introduction

Dilatancy of concentrated suspension is always observed in the appropriate shear rate range when the dispersed solid particles are nonaggregating (Barnes, 1989). Although there are many studies on critical shear rate for the onset of shear thickening and the controlling parameters, size distribution effects on the flow curve has not been paid much attention by most researchers except Alince and Lepoutre (1983). Further, there can not be seen any physical model to predict the dilatant flow curve. On the other hand, there exist many studies on the suspension viscosity probably disregarding its shear thickening or shear thinning properties, or excluding the range in which such properties can be seen significantly. The viscosity dependency on volume fraction of particles, the diameter, and so on, has been discussed also assuming monodisperse particles even if they are polydisperse in the strict sense.

In our previous work (Ookawara and Ogawa, 2000), a new physical model was proposed for the quantitative prediction of dilatant flow curve of suspension in which dispersed particles were also assumed to be monodsiperse. The monodisperse model simply assumes that the momentum transport induced per collision is equal to the momentum difference between particles. In the subsequent study (Ookawara and Ogawa, 2002a), we proposed the expanded model for discrete polydisperse particles such as bimodal and trimodal distributions. In the latest work (Ookawara and Ogawa, 2002b), continuous polydisperse model was presented by mathematical expansion of the discrete model. It is shown that the continuous model gives relations between the viscosity and parameters of representative particle size distributions such as log-normal, Rosin-Rammler distributions and so on.

Since most parameters included in our model were varied independently in the work of Clarke (1967), his experimental data was utilized for verification of the monodisperse model. The particle size of each portion is indicated by maximum and minimum diameters as listed in Table 1. Since we did not incorporate the size distribution effect into the monodisperse model, arithmetical mean of them were utilized as characteristic diameter of monodisperse particles (Ookawara and Ogawa, 2000). In the present study, therefore, more precise verification of our physical model is performed by applying the continuous polydisperse model to the data of Clarke (1967).

*Corresponding author: sokawara@chemeng.titech.ac.jp

2. Constitutive model equation

2.1. Monodisperse model

The monodisperse model assumes that each rigid particle dispersed in a suspension moves at velocity of fluid layer flowing at a given shear rate, in which each particle center exists, without aggregation, Brownian motion, rotational motion. If certain two particles exist in different but adjacent laminar flow layers, they collide at relative velocity that is proportional to the shear rate and length between layers. The momentum difference between those two particles is transported from a fluid layer in which faster particle exists, to the adjacent layer in which slower particle is contained. The summation of momentum transported through control unit area is regarded as the increase of momentum flux that results in viscosity augmentation. Based on the model, the increased momentum flux $\tau_{collison}$ [Pa] is expressed as;

$$\tau_{collision} = k\rho_p D^7 L^2 \dot{\gamma}^2 \tag{1}$$

where k [m], ρ_p [kg/m^3], D [m], L [1/m^3], and $\dot{\gamma}$ [s^{-1}] are arbitrary experimental coefficient, density, diameter and number density of particle, and shear rate, respectively.

2.2. Discrete and continuous polydisperse models

The discrete polydisperse model assumes that suspension particles consist of M monodisperse portions whose diameters are D_1, D_2, ..., D_i, ..., D_M [m], and whose number densities are L_1, L_2, ..., L_i, ..., L_M [1/m^3], respectively. Based on the same assumption of collision, the increase of momentum flux τ_{total} [Pa] is expressed as;

$$\tau_{total} = k\rho_p \dot{\gamma}^2 \sum_{i=1}^{M}\sum_{j=1}^{M} L_j D_j^3 L_j D_{ji}^4 \tag{2}$$

where D_{ji} [m] is radius of imaginary collision sphere defined for the calculation of collision frequency as;

$$D_{ji} = \frac{D_j + D_i}{2} \tag{3}$$

Subscripts i and j are indices to distinguish the particles inside and outside of a shell defined for momentum balance.

The limit as M tends to infinity converges to integral form, viz., continuous polydisperse model as;

$$\tau_{total} = k\rho_p \dot{\gamma}^2 \left(\frac{N}{100V}\right)^2 \int_0^{100}\int_0^{100} dn_j D_j^3 dn_i D_{ji}^4 \tag{4}$$

where N is total particle number dispersed in a suspension whose volume is V [m^3], and n [%] is cumulative percentage undersize by number, respectively. This equation makes it possible to estimate the increased momentum flux for any distribution expressed by continuous function.

Table 1. Particle size range given by Clarke(1967). The density is 2,580 kg/m^3 for quartz particles of all sizes. For D_a=64.5 μm, other three types of sphere particles were used, whose densities are 1,168, 2,360 and 2,960 kg/m^3, respectively. The detail specification is listed in the previous work (Ookawara and Ogawa, 2000)

Particle size range [μm]	D_a [μm]	$C_V=\sigma/D_a$ [-]	$\mu_b^*(C_V)$ [-]
152-211	181.5	0.094	1.05
104-152	128	0.108	1.07
76-104	90	0.090	1.05
53- 76	64.5	0.103	1.06
10- 44	27.0	0.364	1.55

Table A1. Tyler standard sieve series

Tyler mesh	Opening [μm]
60	246
65	208
80	175
100	147
115	124
150	104
170	89
200	74
250	61
270	53
325	43
400	38

Table A2. U.S. sieve series

Sieve No.	Opening [μm]
60	250
70	210
80	177
100	149
120	125
140	105
170	88
200	74
230	62
270	53
325	44

2.3. Suspension with uniform particle size distribution

As shown in Table 1, size of particles used by Clarke (1967) is indicated by each distribution range. Referring to the specification, especially underlined values, of Tyler standard sieve series (Table A1) and U.S. sieve series (Table A2), it seems that he used some kind of sieve series to obtain the particles. Since it is expected that particle size distribution of any portion obtained through screening, is of more uniform than that of original mixture, completely

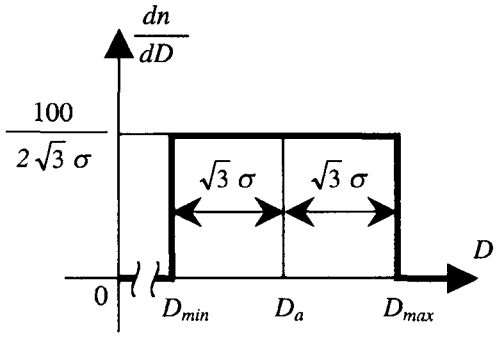

Fig. 1. Uniform particle size distribution assumed to be obtained through screening.

uniform size distribution is reasonably assumed in this study. Figure 1 shows the assumed number size distribution that is constant in the range of minimum diameter D_{min} [m] to maximum diameter D_{max} [m]. For such a uniform distribution, mean diameter D_a [m] and standard deviation σ [m] are expressed as;

$$D_a = \frac{D_{min}+D_{max}}{2} \tag{5}$$

and

$$\sigma = \frac{D_{max}-D_{min}}{2\sqrt{3}} \tag{6}$$

The cumulative percentage undersize by number n [%] is expressed as;

$$n = \begin{cases} \dfrac{100}{2\sqrt{3}\sigma}(D-D_{min}) & (D_{min} \le D \le D_{max}) \\ 0 & (D \le D_{min}) \\ 100 & (D \ge D_{max}) \end{cases} \tag{7}$$

and size distribution is;

$$\frac{dn}{dD} = \begin{cases} \dfrac{100}{2\sqrt{3}\sigma} & (D_{min} \le D \le D_{max}) \\ 0 & (D < D_{min}, D > D_{max}) \end{cases} \tag{8}$$

Eq. (8) makes it possible to change the integral variable n in Eq. (4) to D as;

$$\tau_{total} = k\rho_p\dot{\gamma}^2\left(\frac{N}{2\sqrt{3}\sigma V}\right)^2 \int_{D_{min}}^{D_{max}}\int_{D_{min}}^{D_{max}} D_j^3 D_{ji}^4 dD_j dD_i \tag{9}$$

By using D_a and coefficient of variation;

$$C_V = \frac{\sigma}{D_a} \tag{10}$$

Eq. (9) is calculated as;

$$\tau_{total} = k\rho_p\dot{\gamma}^2\left(\frac{N}{V}\right)^2 D_a^7\left(1+12C_V^2+24C_V^4+\frac{54}{7}C_V^6\right) \tag{11}$$

Since mean volume diameter D_V [m] is also calculated as;

$$D_V = \left(\frac{\int_0^{100} dnD^3}{\int_0^{100} dn}\right)^{\frac{1}{3}} = D_a\sqrt[3]{1+3C_V^2} \tag{12}$$

Eq. (11) is rewritten by using volume fraction of particles C and volume shape factor ϕ_v as;

$$\tau_{total} = k_V\rho_p\dot{\gamma}^2C^2D_a\mu_b^*(C_V) \tag{13}$$

where

$$k_V = \frac{k}{\phi_V^2} \tag{14}$$

and

$$\mu_b^*(C_V) = \frac{1+12C_V^2+24C_V^4+\frac{54}{7}C_V^6}{(1+3C_V^2)^2} \tag{15}$$

Eventually, flow curve of the suspension is expressed as

$$\tau = \{\mu_0 + k_V\rho_pC^2\dot{\gamma}D_a\mu_b^*(C_V)\}\dot{\gamma} \tag{16}$$

where μ_0 is the continuous phase viscosity. Further, suspension viscosity is expressed as;

$$\mu = \mu_0 + k_V\rho_pC^2\dot{\gamma}D_a\mu_b^*(C_V) \tag{17}$$

The term $\mu_b^*(C_V)$ is additionally contained in this equation compared with the monodisperse model. By means of this term, the influence of distribution width on flow curve can be analyzed independent of average diameter. Additionally, the term can be regarded as correction coefficient for polydisperse particles to simulate monodisperse particles whose diameter is regarded as $D_a\mu_b^*(C_V)$. In other words, the product of D_a and $\mu_b^*(C_V)$ corresponds to the diameter of monodisperse particles that results in same viscosity increase. Since Eq. (17) converges to the monodisperse model as C_V tends to 0, incidentally, it can be said this model is mathematically consistent with previous models.

Figure 2 shows the relation between C_V and $\mu_b^*(C_V)$. The relation between geometric standard deviation σ_g and $\mu_{log}^*(\sigma_g)$ (Ookawara and Ogawa, 2002b) is also shown because of the similarity of both indices for the distribution width, viz., the both values of (C_V+1) and σ_g correspond to the ratio $D_{u84.13}/D_{50}$. Herein, $D_{u84.13}$ and D_{50} are diameters where each cumulative undersize is 84.13% and 50%, respectively. The physical significance of $\mu_{log}^*(\sigma_g)$ is equal to that of $\mu_b^*(C_V)$ abovementioned. It can be seen that both functions increase exponentially with the indices. The function $\mu_b^*(C_V)$, however, shows relatively slower increase than $\mu_{log}^*(\sigma_g)$. This is because of mathematically infinite integral range of log-normal distribution including the effect of larger particles compared with uniform distribution. It can be seen that, to the contrary, the function value is kept less than 1.05 and can be regarded as nearly constant in the C_V range of below 0.1. Since any proper sieve series has sufficiently small opening differences as listed in Tables A1 and A2, C_V of any portion obtained by

screening, except top and bottom, is sufficiently small as shown in Table 1. Therefore, such portion could be regarded as monodisperse from the viewpoint of our suspension viscosity model.

3. Verification

The coefficient k_V in Eq. (17) should be determined by experiments since it is assumption that the momentum transported between fluid layers per collision is equal to the momentum difference between particles. For the verification of derived equation, therefore, experimental data of Clarke (1967) is cited in this study since controlling parameters, viz., density and diameter of particle, shear rate, and volume fraction, were varied independently in his work.

If viscosity dependency on each parameter can be described by a unique value of k_V in a particular range, that is the very range in which the model can be regarded as valid practically. The unique value is denoted by k_U in this study. Subsequently to the determination of k_U, the model predicts a linear increase of viscosity with shear rate, viz., dilatant flow characteristics. Further, the increase of viscosity is expected to be proportional to the square of volume fraction, and to show the linear dependency on density and diameter of particle.

Since viscosity measurement was performed at 25.0± 0.1°C in his study, viscosity of disperse medium, which is water, is set to 0.000894 Pa·s in the following discussion. Further, the values of all symbols in the following figures are read from the figures in his work.

3.1. Suspension of quartz particle

Figure 3 shows the viscosity dependency on shear rate in the range of 109.7 to 327.7 s^{-1} for quartz particles, whose density, average diameter and volume fraction range are 2,580 kg/m^3, 181.5×10^{-6} m and 0.05 to 0.30, respectively. Substitution of these known values for parameters in Eq. (17) yields Eq. (18) as follows.

$$\mu = 0.000894 + k_V[(2,580)(181.5\times10^{-6})(1.05)(0.05^2\cdots0.30^2)]\dot{\gamma} \quad (18)$$

The comparison of Eq. (18) with the results of curve fit gives k_V value for each volume fraction as listed in Table 2. Coefficients for the monodisperse model are also shown for the comparison. Since the value of $\mu_b^*(C_V)$ is constant in this case, k_V is simply 1.05 times as k. It can be seen that k_V values marked by asterisk are similar to each other in volume fraction range of 0.15 to 0.25. On the other hand, other k_V values increase as volume fraction goes away from this range. In the following Figs. 3-6, broken lines are drawn by using unmarked k_V values listed in the corresponding tables and solid lines are drawn by k_U, which is average of marked k_V and the value is 0.00181 m for quartz particle in this study. It can be seen in Fig. 3 that it is possible to estimate viscosity change by using the unique value of k_U in the above concentration and shear rate ranges. It should be noted, further, broken lines also fit the plots very well in spite that k_V values are considerably different from k_U value.

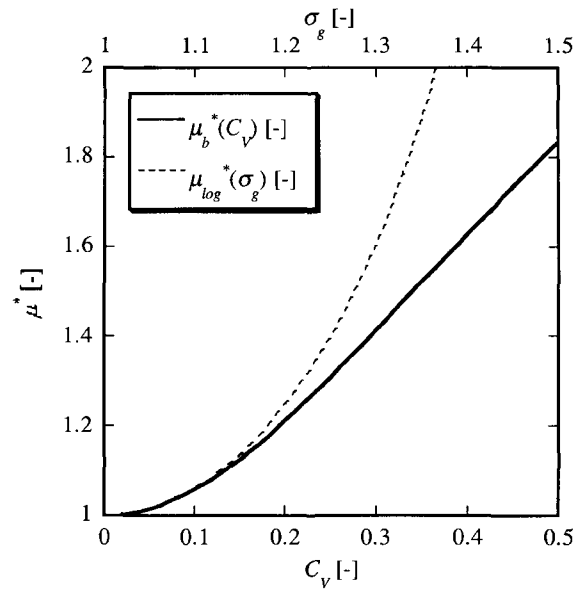

Fig. 2. Comparison between non-dimensional functions $\mu_b^*(C_V)$ based on uniform distribution and $\mu_{log}^*(\sigma_g)$ based on log-normal distribution.

Table 2. The values of parameter k_V [mm] calculated based on the viscosity dependency shown in Fig. 3

C [-]	k_V [mm]	k [mm]
0.05	7.09	7.44
0.10	2.72	2.85
0.15	*1.88	1.97
0.20	*1.74	1.82
0.25	*1.77	1.85
0.275	2.43	2.55
0.30	3.70	3.88

Figure 4 shows the viscosity dependency at shear rate of 216.6 s^{-1} on the corrected diameter $D_a\mu_b^*(C_V)$ for quartz particles, whose volume fraction range is 0.10 to 0.30. Substitution of these known values for parameters in Eq. (17) yields Eq. (19) as follows.

$$\mu = 0.000894 + k_V[(2,580)(0.10^2\cdots0.30^2)(216.6)]D_a\mu_b^*(C_V) \quad (19)$$

The comparison of Eq. (19) with the results of curve fit gives k_V value for each volume fraction as listed in Table 3. Coefficients for the monodisperse model are also shown for the comparison. It can be seen that k_V values marked by asterisk are also similar to each other in the concentration

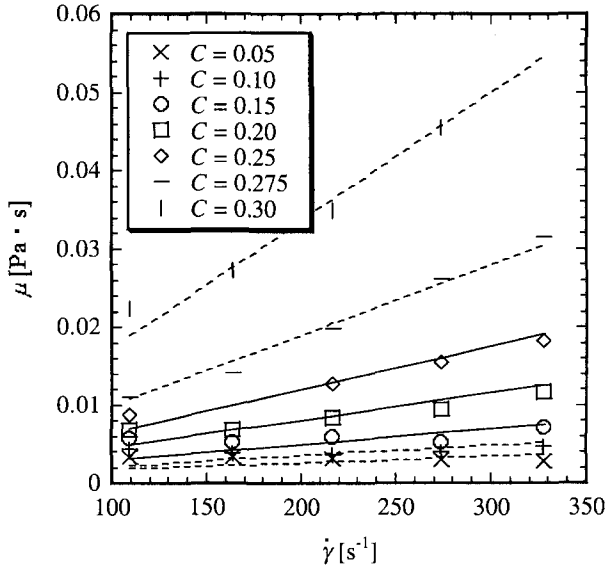

Fig. 3. Viscosity increase with shear rates for quartz particle suspensions. (ρ_p=2,580 kg/m^3; D_a=181.5 μm; $\mu_b^*(C_V)$=1.05; C=0.05-0.30; μ_0=0.000894 Pa·s).

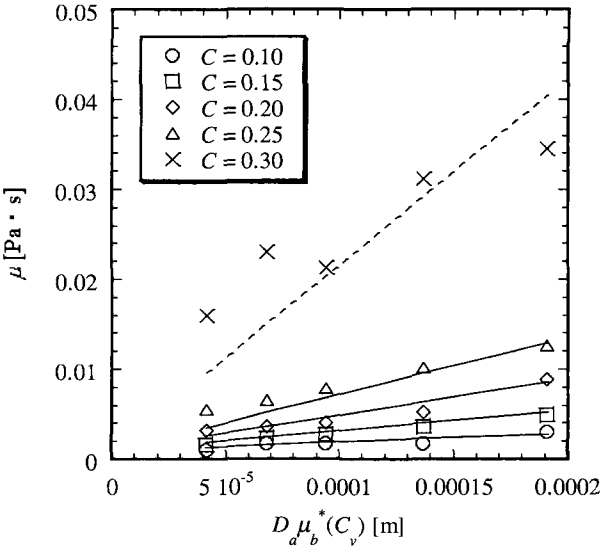

Fig. 4. Viscosity increase with corrected diameter $D_a\mu_b^*(C_V)$ for quartz particle suspensions. (ρ_p=2,580 kg/m^3; C=0.05-0.30; $\dot{\gamma}$=216.6 s^{-1}; μ_0=0.000894 Pa·s).

Table 3. The values of parameter k_V [mm] calculated based on the viscosity dependency shown in Fig. 4

C [-]	k_V [mm]	k [mm]
0.10	*1.71	1.83
0.15	*1.65	1.75
0.20	*1.70	1.80
0.25	*1.94	2.04
0.30	4.13	4.35

Table 4(a). The values of parameter k_V [mm] calculated based on the viscosity dependency shown in Fig. 5

D_a [μm]	k_V [mm] C:0.10-0.20	k_V [mm] C:0.10-0.25	k_V [mm] C:0.10-0.30
27	#*2.09	2.81	5.30
64.5	*1.77	2.17	4.59
90	1.52	*1.90	3.27
128	1.44	*1.76	3.26
181.5	1.83	*1.78	2.77

Table 4(b). The values of k obtained by assuming monodisperse distribution (Ookawara and Ogawa, 2000)

D_a [μm]	k [mm] C:0.10-0.20	k [mm] C:0.10-0.25	k [mm] C:0.10-0.30
27	3.25	4.35	8.21
64.5	1.88	2.30	4.87
90	1.59	2.00	3.42
128	1.54	1.89	3.49
181.5	1.92	1.87	2.91

range of 0.10 to 0.25, and also similar to values marked by asterisk in Tables 2 and 4(a). As shown in Fig. 4, plots deviate upward from the fitted line in the smaller diameter range. However, the extent of deviation is much smaller compared with the monodisperse model (Ookawara and Ogawa, 2000). This is because large $\mu_b^*(C_V)$ value caused by large C_V value of smallest portion moves the plot rightward to fitting line that must pass through fixed point, viz., 0.000894 at D_a=0. Therefore, it can be said that newly introduced term $\mu_b^*(C_V)$ expands the applicable range of the model compared with the monodisperse model.

Figure 5 shows the viscosity dependency at shear rate of 216.6 s^{-1} on volume fraction in the range of 0.1 to 0.3 for quartz particles, whose average diameter range is 27 to 181.5 μm. Substitution of these known values for parameters in Eq. (17) yields Eq. (20) as follows.

$$\mu = 0.000894 + k_V[(2,580)(216.6)(27.5\times10^{-6} \times 1.55\cdots181.5\times10^{-6}\times1.05)]C^2 \quad (20)$$

Since it seems that viscosity dependency on volume fraction varies gradually and viscosity increases exponentially rather than proportionally to the square of volume fraction, especially in the higher range, curve fit is examined in three different ranges, viz., 0.10-0.20, 0.10-025 and 0.10-0.30, respectively. The comparison of Eq. (20) with the results of curve fit gives k_V value for each average diameter and fitting range as listed in Table 4(a). Coefficients for the monodisperse model are also listed in Table 4 (b) for the comparison. As shown in Table 4(a), similar values marked

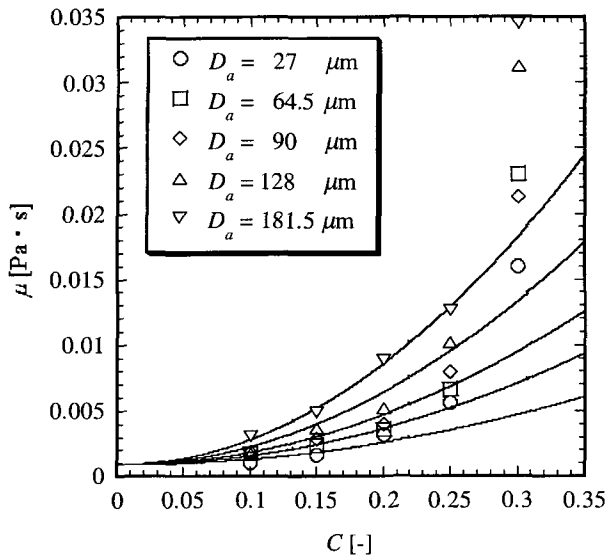

Fig. 5. Viscosity increase with volume fraction for quartz particle suspensions. (ρ_p=2,580 kg/m^3; $\dot{\gamma}$=216.6 s^{-1}; $D_a \cdot \mu_b^*(C_V)$= (27)(1.55)-(181.5)(1.05) μm; μ_0=0.000894 Pa·s).

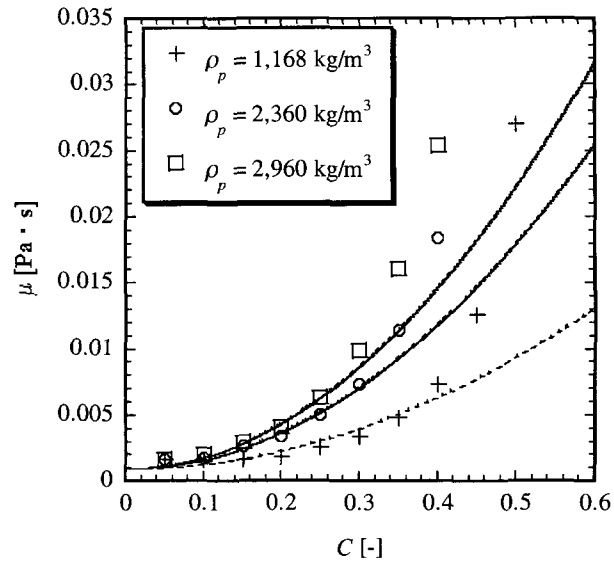

Fig. 6. Viscosity increase with volume fraction for sphere particle suspensions. (ρ_p=1,168-2,960 kg/m^3; $\dot{\gamma}$=327.7 s^{-1}; $D_a \cdot \mu_b^*(C_V)$=(64.5)(1.06) μm; μ_0=0.000894 Pa·s).

by asterisk can be seen in different columns. For diameter of 27.5 and 64.5, the values fitted in the volume fraction range of 0.10 to 0.20, are similar to the marked values listed in Tables 2 and 3. For the diameter range of 90 to 181.5 μm, on the other hand, proper values appear when curve fit is performed in the volume fraction range of 0.10 to 0.25. The fact implies that the upper limit of valid volume fraction range is raised with average diameter. Further, it can be seen for the smallest portion that k_V value marked by # in Table 4(a) is much improved compared with a corresponding value in Table 4(b). This improvement is achieved by the large $\mu_b^*(C_V)$ value caused by large C_V value. Therefore, it can be emphasized again that newly introduced term $\mu_b^*(C_V)$ expands the applicable range of the model compared with the monodisperse model.

3.2. Suspension of sphere particle that consist of glass or polymethlmethacrylate

Figure 6 shows the viscosity dependency at shear rate of 327.7 s^{-1} on volume fraction in the range of 0.05 to 0.45 for sphere particles, whose diameter and density range is 64.5 μm and 1,168 to 2,960 kg/m^3, respectively. Substitution of these known values for parameters in Eq. (17) yields Eq. (21) as follows.

$$\mu = 0.000894 + k_V[(1,168 \cdots 2,960)(327.7)(64.5\times10^{-6})(1.06)]C^2 \quad (21)$$

Referring to applicable volume fraction range for quartz particles and the values listed in the following Table 6 to obtain similar k_V values as much as possible, curve fit is performed in the volume fraction range of 0.05 to 0.25. The comparison of Eq. (21) with the results of curve fit

Table 5. The values of parameter k_V [mm] calculated based on the viscosity dependency shown in Fig. 6

ρ_p [kg/m^3]	k_V [mm]
1,168	1
2,360	*1.24
2,960	*1.28

Table 6. The values of parameter k_V [mm] calculated based on the viscosity dependency shown in Fig. 7

C [-]	k_V [mm]
0.05	5.71
0.10	1.75
0.15	*1.42
0.20	*1.16
0.25	*1.25
0.30	*1.41
0.40	*1.31
0.45	1.70

gives k_V value for each density as listed in Table 5. Since the value of $\mu_b^*(C_V)$ is constant in this case, k_V is simply 1.06 times as k for the monodisperse model. It can be seen that marked k_V values for density of 2,360 and 2,960 kg/m^3 are similar to each other, but much smaller than values for quartz particles. In Figs. 6 and 7, solid lines are drawn by using k_U, which is average of k_V values marked by asterisk in Tables 5 and 6, and the value is 0.00130 m in this study.

Figure 7 shows the viscosity dependency at shear rate of 327.7 s^{-1} on particle density in the volume fraction range of 0.05 to 0.45 for sphere particles, whose average diameter is

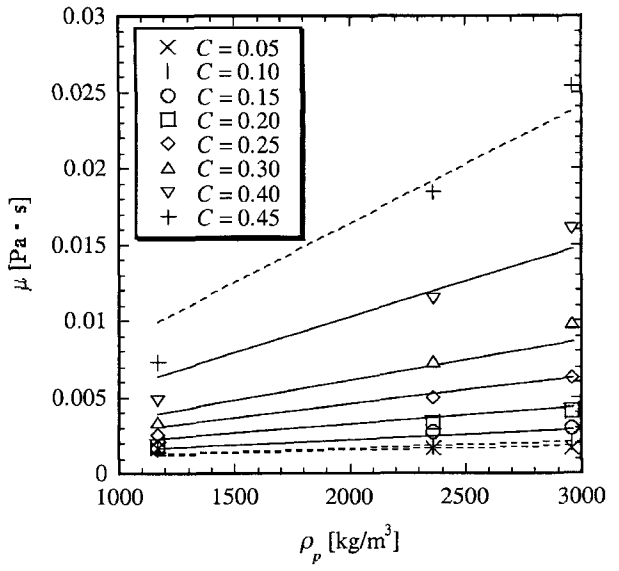

Fig. 7. Viscosity increase with volume fraction for sphere particle suspensions. ($\dot{\gamma}$=327.7 s^{-1}; $D_a \cdot \mu_b^*(C_V)$=(64.5)(1.06) μm; C=0.05-0.45; μ_0=0.000894 Pa·s).

64.5 μm. Substitution of these known values for parameters in Eq. (17) yields Eq. (22) as follows.

$$\mu = 0.000894 + k_V[(327.7)(64.5\times10^{-6})(1.06)(0.05^2\cdots0.45^2)]\rho_p \quad (22)$$

The comparison of Eq. (22) with the results of curve fit gives k_V value for each density as listed in Table 6. Since the value of $\mu_b^*(C_V)$ is also constant in this case, k_V is simply 1.06 times as k for the monodisperse model. It can be seen that marked k_V values are similar to each other in the volume fraction range of 0.15 to 0.40 and to marked values in Table 5.

3.3. Discussion

As shown in Figs. 3-5 and corresponding Tables 2, 3 and 4(a), it is confirmed that the model is valid for quartz particles, in the volume fraction range of 0.15 to 0.25, in the shear rate range of 109.7 to 327.7 s^{-1} and in the diameter range of 27 to 181.5 μm. For sphere particles, on the other hand, it is verified that the model is valid in the volume fraction range of 0.05 to 0.20 and in the density range of 2,360 to 2,960 kg/m^3 as shown in Figs. 6 and 7 and corresponding Tables 5 and 6. Although these ranges are almost same as those for the monodisperse model, a newly introduced correction term $\mu_b^*(C_V)$ definitely expands the applicable diameter range and fitting is improved as shown in Figs. 4 and 5. It should be noted, further, the plots are fitted well even out of above mentioned ranges. It is suggested, therefore, the model is practically applicable not only in the confirmed range, but also over the broader range by using the particular k_V value, which is valid only in the particular narrow range.

4. Conclusion

In this study, it is assumed that particle size distribution of any portion obtained through screening is practically uniform. Therefore, a new relation between parameters of the uniform distribution, viz., average diameter and coefficient of variation, and the flow characteristics of suspension is derived based on the continuous polydisperse model (Ookawara and Ogawa, 2002b). The derived model equation predicts a linear increase of viscosity with shear rate, viz., dilatant flow characteristics. Further, the increase of viscosity is expected to be proportional to the square of volume fraction of particles, and to show the linear dependency on density and average diameter of particles. It is also shown that the uniform distribution model includes additional term that expresses the effect of distribution width. For verification of the model, experimental results of Clarke (1967) are cited as well as in our previous work for the monodisperse model (Ookawara and Ogawa, 2000) since most parameters were varied independently in his work. Curve fits to those data based on the model determined experimental constants for each condition. Some of them are similar to each other in particular experimental ranges. In this study, it is concluded that those are the very ranges in which the model is valid practically. Further, it is confirmed that a unique value of the constant, which is average of aforementioned similar values, could correlate the viscosity dependency on all factors in the ranges. It is also verified that the newly introduced term expands the applicable range compared with the monodisperse model.

References

Alince, B. and P. Lepoutre, 1983, Flow behavior of pigment blends, *Tappi Journal* **66**, 57-60.

Barnes, H. A., 1989, Shear-thickening ("Dilatancy") in suspensions of nonaggregating solid particles dispersed in Newtonian liquids, *Journal of Rheology* **33**, 329-366.

Clarke, B., 1967, Rheology of coarse settling suspensions, *Trans. Instn. of Chem. Engrs.* **45**, T251-T256.

Ookawara, S. and K. Ogawa, 2000, Shear thickening flow characteristics model of suspensions, *Kagaku Kogaku Ronbunshu* **26**, 366-373.

Ookawara, S. and K. Ogawa, 2002a, Theoretical study on particle size distribution and suspension viscosity, *Kagaku Kogaku Ronbunshu* **28**, 322-329.

Ookawara, S. and K. Ogawa, 2002b, Relation between suspension viscosity and parameter of representative particle size distribution, *Kagaku Kogaku Ronbunshu* **28**, 779-784.